Research Article | Vol. 25, No. 21 | 16 Oct 2017 | OPTICS EXPRESS 25970
Optics EXPRESS

Directed and non-reciprocal transport in linear and ring dynamic quantum networks and width-patterned optical waveguide arrays

CLARA JAVAHERIAN* AND JASON TWAMLEY

ARC Centre for Engineered Quantum Systems, Department of Physics and Astronomy, Macquarie University, Sydney, NSW 2109, Australia
*Clara.Javaherian@mq.edu.au

Abstract: Non-reciprocal and uni-directional transport could efficiently transmit signals in integrated quantum and optical networks. Dynamic quantum nodes and optical waveguide arrays are proposed in linear and ring configurations for directed and non-reciprocal transport. It is shown that the time-dependent modulation of the position of quantum nodes in linear arrays would efficiently and non-reciprocally guide an initially injected quantum energy. The initial energy could be trapped within a ring configuration of such dynamically controlled quantum nodes. In linear parallel waveguide arrays, fashioning the widths pattern could also uni-directly transfer Gaussian beams across the arrays. By arranging the parallel waveguides on a cylindrical shell with a new widths pattern, the uni-chiral transport of Gaussian beams is achieved.

OCIS codes: (230.5590) Quantum-well, -wire and -dot devices; (080.1238) Array waveguide devices; (060.5565) Quantum communications.

References and links

1. M. D. Tocci, M. J. Bloemer, M. Scalora, J. P. Dowling, and C. M. Bowden, "Thin-film nonlinear optical diode," Appl. Phys. Lett. **66**, 2324 (1995).
2. V. V. Konotop, and V. Kuzmiak, "Nonreciprocal frequency doubler of electromagnetic waves based on a photonic crystal," Phys. Rev. B **66**, 235208 (2002).
3. J. Ren, J. X. Zhu, "Theory of asymmetric and negative differential magnon tunneling under temperature bias: Towards a spin Seebeck diode and transistor," Phys. Rev. B **88**, 094427 (2013).
4. J. Ren, "Predicted rectification and negative differential spin Seebeck effect at magnetic interfaces," Phys. Rev. B **88**, 220406(R) (2013).
5. S. S. Mathur, and M. S. Sagoo, "Rectification of acoustic waves," Can. J. Phys. **52**(17), 1726–1730 (1974).
6. B. Liang, B. Yuan, and J. C. Cheng, "Acoustic Diode: Rectification of Acoustic Energy Flux in One-Dimensional Systems," Phys. Rev. Lett. **103**, 104301 (2009).
7. S. Longhi, "Non-reciprocal transmission in photonic lattices based on unidirectional coherent perfect absorption," Opt. Lett. **40**(7), 1278–1281 (2015).
8. N. Li, and J. Ren, "Non-reciprocal geometric wave diode by engineering asymmetric shapes of nonlinear materials," Sci. Rep. **4**, 6228 (2014).
9. Y. Shen, M. Bradford, and J. T. Shen, "Single-photon diode by exploiting the photon polarization in a waveguide," Phys. Rev. Lett. **107**, 173902 (2011).
10. K. Xia, G. Lu, G. Lin, Y. Cheng, Y. Niu, S. Gong, and J. Twamley, "Reversible nonmagnetic single-photon isolation using unbalanced quantum coupling," Phys. Rev. A **90**, 043802 (2014).
11. L. D. Tzuang, K. Fang, P. Nussenzveig, S. Fan, and M. Lipson, "Non-reciprocal phase shift induced by an effective magnetic flux for light," Nature Photon. **8**(9), 701–705 (2014).
12. K. Fang, Z. Yu, Z. Yu, and S. Fan, "Photonic Aharonov-Bohm effect based on dynamic modulation," Phys. Rev. Lett. **108**, 153901 (2012).
13. W. Smigaj, J. Romero-Vivas, B. Gralak, L. Magdenko, B. Dagens, and M. Vanwolleghem, "Magneto-optical circulator designed for operation in a uniform external magnetic field," Opt. Express **35**(4), 568-570 (2010).
14. M. Tien, T. Mizumoto, P. Pintus, H. Kromer, and J. E. Bowers, "Silicon ring isolators with bonded nonreciprocal magneto-optic garnets," Opt. Express **19**(12), 11740–11745 (2011).
15. L. Bi, J. Hu, P. Jiang, D. H. Kim, G. F. Dionne, L. C. Kimerlin, and C. A. Ross, "On-chip optical isolation in monolithically integrated non-reciprocal optical resonators," Nature. Photon. **5**, 758–762 (2011).
16. Z. Yu, and S. Fan, "Optical isolation: A non-magnetic approach," Nature. Photon. **5**, 517–519 (2011).
17. L. Yuan, S. Xu, and S. Fan, "Achieving nonreciprocal unidirectional single-photon quantum transport using the photonic Aharonov Bohm effect," Opt. Lett. **40**(22), 5140 (2015).

#294789 https://doi.org/10.1364/OE.25.025970
Journal © 2017 Received 10 May 2017; revised 27 Jul 2017; accepted 30 Jul 2017; published 11 Oct 2017

Optics EXPRESS

18. E. Lenferink, G. Wei, and N. P. Stern, "Coherent optical non-reciprocity in axisymmetric resonators," Opt. Express **22**(13), 16099–16111 (2014).
19. S. Longhi, "Aharonov-Bohm photonic cages in waveguide and coupled resonator lattices by synthetic magnetic fields," Opt. Lett. **39**(20), 5892 (2014).
20. S. Longhi, "Effective magnetic fields for photons in waveguide and coupled resonator lattices," Opt. Lett. **38**(18), 3570–3573 (2013).
21. C. Monroe and J. Kim, "Scaling the Ion Trap Quantum Processor," Science **339**, 1164–1169 (2013).
22. A. B. Hall, S. L. Coy, A.Kafle, J. Glick, E. Nazarov, and P. Vouros, "Extending the Dynamic Range of the Ion Trap by Differential Mobility Filtration," Am Soc Mass Spectrom. **24**(9), 1428–1436 (2013).
23. J. Sebby-Strabley, M. Anderlini, P. S. Jessen, and J. V. Porto, "Lattice of double wells for manipulating pairs of cold atoms," Phys. Rev. A **73**, 033605 (2006).
24. M. Anderlini, J. Sebby-Strabley, J. Kruse, J. V. Porto, and W. D. Phillips, "Controlled atom dynamics in a double-well optical lattice," J. Phys. B: At. Mol. Opt. Phys. **39**, S199–S210 (2006).
25. A. Stone, H. Jain, V. Dierolf, M. Sakakura, Y. Shimotsuma, K. Miura, K. Hirao, J. Lapointe, and R. Kashyap, "Direct laser-writing of ferroelectric single-crystal waveguide architectures in glass for 3D integrated optics," Sci. Rep. **5**, 10391 (2015).
26. G. D. Marshall, A. Politi, V. Dierolf, M. Sakakura, Y. Shimotsuma, K. Miura, K. Hirao, J. Lapointe, and R. Kashyap, "Laser written waveguide photonic quantum circuits," Opt. Express **17**(15), 12546–12554 (2009).
27. C. Javaherian, "Quantum transport and switching in long-range coupled quantum systems," (Ph.D. thesis, Macquarie University, Sydney, Australia, 2016), Chap. 2.
28. J. Poulin, P. S. Light, R. Kashyap, and A. N. Luiten, "Optimized coupling of cold atoms into a fiber using a blue-detuned hollow-beam funnel," Phys. Rev. A **84**, 053812 (2011).
29. T. Hartmann, F. Keck, H. J. Korsch, and S. Mossmann, "Dynamics of Bloch oscillations," New J. Phys. **6**, 2 (2004).
30. R. Morandotti, U. Peschel, J. S. Aitchison, H. S. Eisenberg, and Y. Silberberg, "Experimental Observation of Linear and Nonlinear Optical Bloch Oscillations," Phys. Rev. Lett. **83**(23), 4756–4759 (1999).
31. P. D. McIntyre, and A. W. Snyder, "Power transfer between optical fibers," J. Opt. Soc. Am. **63**(12), 1518–1527 (1973).

1. Introduction

Non-reciprocal asymmetric transport is a highly desirable feature in integrated quantum photonics networks, and could be used in designing isolators, circulators, or quantum/optical diodes. This feature has been achieved for different wave types such as optical waves [1,2], spin waves [3,4], and acoustic waves [5,6]. Isolators, diodes, and circulators have been fashioned through different spatial dimensions i.e. 2D and 3D planer arrays of waveguides [1,3,7,8], 1D linear systems [9,10], and a combination of 1D and 2D networks [8]. Uni-directional transport of optical waves could be achieved by applying magnetic fields [11–15]. While the manipulation of magnetic field is not handy in small networks, non-magnetic non-reciprocal transport has been investigated [8, 10, 16] for integrated systems. Regarding non-reciprocal photon transport, there are many theoretical proposals [12, 17–20], and experimental demonstrations of non-reciprocal phase shifts [18]. In [17] Yuan et al used photonic Aharonov Bohm effect to obtain non-reciprocal uni-directional single-photon transport to demonstrate quantum information processing tasks [9, 10, 18]. A different route towards realizing asymmetric transport in discrete optical systems is proposed in [7] through a dissipative Aharonov Bohm diode. They considered an effective magnetic field introduced by periodic modulation of optical parameters [12, 19, 20] that is a technique using for linear lattices with no nonlinear or magnetic media.

In this work we propose different dynamic or static networks to be used for non-magnetic uni-directional transport in small integrated circuits. The networks are expanded in various spatial dimensions and designed for non-reciprocal transport of quantum-carriers and Gaussian beams. They could be implemented by different site-based dynamic networks like ion traps [21, 22] and waveguide arrays [20] to be used in quantum or optical integrated networks. The two transportation mechanisms in such networks are energy oscillation within sites whose positions could be dynamic, and optical tunneling within spatially modulated optical waveguides. For dynamic site designs, we consider a scheme where the energy excitation is uni-directionally transported within the network via the dynamical close proximity of pairs of sites. We initially study a linear array of moving sites. The proposed dynamic networks could be implemented

Optics EXPRESS

either as curved optical waveguides or cold atoms trapped in dynamic optical lattices [23, 24]. We then wrap up the dynamic linear array to form a close spatial ring and we are able to show that simple oscillatory motions of the individual sites on the ring lead to uni-chiral (clockwise or counterclockwise), transport of energy excitations on the ring via energy oscillation between the sites. The corresponding ring configurations, which could be considered as optical circulators, could be implemented by static curved waveguides on cylindrical substrates or cold atoms trapped in controlled ring optical lattices. We also introduce two methods to achieve non-reciprocal transport within parallel waveguide arrays along planar and cylindrical substrates. For linear planar arrays we consider a sawtooth spatial modulation of the propagation constants via a proposed width pattern of individual waveguides in which the gradient of the width profile periodically flips along the waveguides axes. In this structure we find that an initial Gaussian beam, which would normally propagate as a Bloch oscillation, now experiences a homogenous spatial force which periodically reverses sign and this combination leads the Bloch wave to move in one direction. We again are able to wrap up this linear array into a ring and deduce the spatial modulations of the propagation constants and waveguides widths required to yield non-reciprocal uni-chiral transport on a cylindrical shell of parallel waveguides. All proposed designs could be implemented by static curved or width-pattened waveguide arrays that could be built by direct laser writing of waveguides [25, 26]. So these non-reciprocal non-magnetic directed devices have advantage over magnetic or time-dependent couplings/refractive indices designs.

2. Discussion

To achieve directed transport we consider a next-nearest-sites-interacting system consisting of N sites. The general form of Hamiltonian of the system is $H = \sum_{i=1}^{N_0}(J_{i,i+1}\hat{\sigma}_i^{\dagger}\hat{\sigma}_{i+1} + CC) + \sum_{i=1}^{N}\omega_i\hat{\sigma}_i^{\dagger}\hat{\sigma}_i$, where $J_{i,i+1}$ is the interaction energy of two nearest sites, ω_i is the self-energy of site i, $\hat{\sigma}_i^{\dagger}(\hat{\sigma}_i)$ is the creation (annihilation) operator of an energy excitation on site i, $N_0 = N$ for a ring network where $N + 1^{st}$ site is the first site, and $N_0 = N - 1$ for a linear network. The evolution of this system is determined by equation: $d\phi(q)/dq = -i\alpha H\phi(q)$. Considering $q = t$ and $\alpha = -1/\hbar$, the Schrodinger equation appears with $\phi(t)$ as the total quantum state of the system. On the other hand, by considering $q = z$, $\alpha = 1$, and $\omega_i = \beta_i$ where β_i represents the propagation constant of waveguide i along z axis, the evolution equation turns to the coupled mode equations of a propagating wave through an $N-$waveguide parallel array and $\phi(z) = (a_1(z); ...;a_n(z))$ is a column vector of electric field amplitudes on each waveguide. We now seek suitable Hamiltonians for directed transport in both dynamic site networks and waveguide arrays. In the first part, we consider linear arrays i.e. particles on a line or parallel waveguides on a plane, and find the appropriate conditions to achieve uni-directional transport. In the second part, we couple the first and last sites of the linear arrays to obtain the corresponding ring or cylindrical networks.

2.1. Linear arrays

In this section we introduce two methods to achieve directed and non-reciprocal transport in linear arrays. The first method is represented by a linear array of eight moving sites where the position of each site along x axis as a function of time is shown in Fig. 1(a) and (b). The first and last sites are fixed on x axis while the middle sites start oscillating in due times. The initial separation of sites 1 and 2 is 0.007, the positions of pair of middle sites $i = n$ and $n + 1$, at time t are $x_i = (n/2)a_i + b_i sin(0.08t + \pi - 0.3125\pi(n/2 - 1)) + d_{Block}(n/2 - 1)$; where $(a_n, b_n) = (0.5, 0.495)$, $(a_{n+1}, b_{n+1}) = (0.507, 0.49)$, and $d_{Block} = 1.009$, and the last site is permanently located at $x_N = d_{Block}(N/2 - 1) + 0.005$. We initially launch an energy excitation on the first site, while considering zero self-energies for all sites ($\omega_i = 0$), and dipolar interaction energies between the next nearest sites ($J_{i,i+1} = 1/r_{i,i+1}^3$). We choose these parametrization for the time modulation of the positions of sites to yield at type of trap for the light made from

Optics EXPRESS

pairs of sites that lead to directed motion. We numerically calculated the probabilities of finding energy excitation on each site in time as shown in Fig. 1(c). While assumed $\hbar = 1$, the Planck units could be considered for the physical quantities. It can be seen that the directed energy transport could be achieved via the proposed pattern of dynamic particle network. This is due to the fact that the initial energy excitation on first site which is fixed at the origin would oscillate between sites 1 and 2 in terms of a superposition state. It then transfers along the x axis within the superposition states of different pair of sites in subsequent intervals. In other words, the initial energy follows closely the trajectory of increased interaction energy along the closely located nearest sites, which possesses the lowest eigenenergy of the total network [27]. Such networks could be straightforwardly scaled up by adding pair of sites along the networks, however, one should adjust the start up time of site oscillations in accordance with the network size and the total number of sites.

These dynamically controlled particle networks are non-reciprocal so that by initializing the system on the N^{th} site, the energy excitation spreads over all sites leading to low efficiency of transport towards the first site. It has been checked that such isolators are perfectly non-reciprocal and keep the total incident energy on the N^{th} site, if the initial launching to the last site would be after one network cycle, that is the time by which the last oscillating site ($N-1^{st}$ site) has spanned its geometrical domain for once. A complete reciprocal version of such arrays can be obtained by flipping the dynamic pattern of site positions in time after each network cycle. The proposed particle networks could be implemented by cold atoms in optical lattices [23, 24] and couple to optical beams in larger photonic circuits [28]. In addition, according to the general form of the equation of motion discussed in section 2, such designs could be also implemented by 2D curved optical waveguide arrays with the curvature pattern of Fig. 1. Now we present another

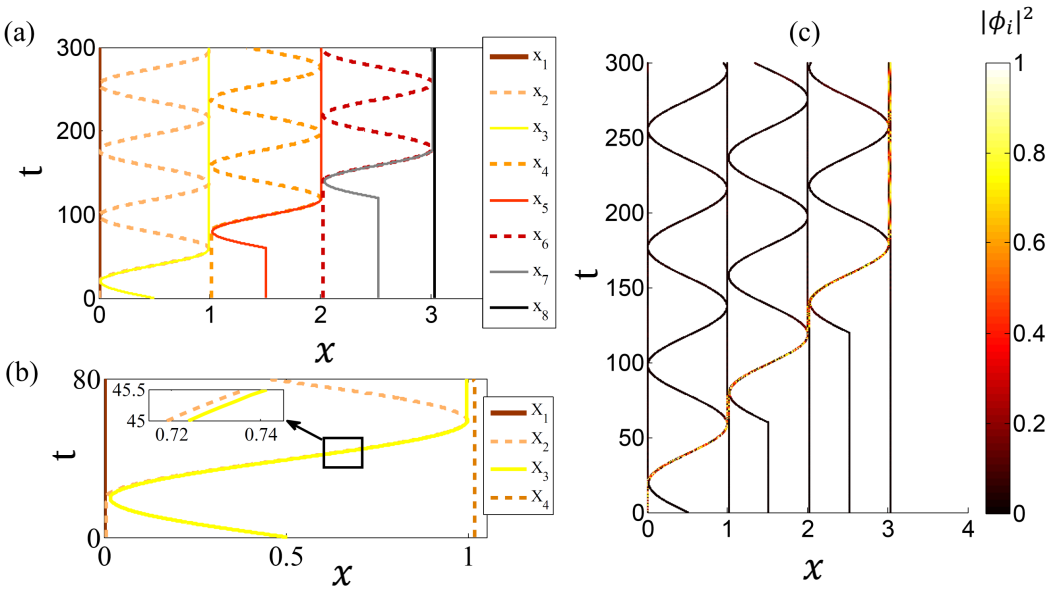

Fig. 1. Graph (a) shows an eight-site one-dimensional network which achieves directed energy transport. x_i is the position of site i along x axis in time. Graph (b) is an enlargement of graph (a) and shows the pair of sites that are close together. Graph (c) is the dynamic evolution of the energy excitation initially located at site 1 at $t = 0$. $|\phi_i|^2$ is the probability of finding the energy excitation on site i at various times. Due to the pattern of pairing of the sites, the energy excitation moves in a directed fashion to the right.

method of directed transport in parallel waveguide arrays. The uni-directional transport of a

Optics EXPRESS

Gaussian beam has been previously achieved in a tight binding model by the periodic flipping in time of an electric force applied across a next nearest sites interacting 1D lattice [29]. We consider a more detailed implementation of this concept using a linear optical waveguide array whose widths vary along z axis to effect equivalent to the periodic flipping of a homogenous electric force. An alternative to design waveguides width profile would be to fashion the waveguides from electro-optic materials and apply a different z-dependent electric field along each waveguide to yield a modulated homogenous force on the Bloch oscillating Gaussian beam resulting in non-reciprocal transport. A lateral increase in waveguides widths in a parallel array changes the propagation constants of individual waveguides (a schematic shown on a line on top of Fig. 1(a) in [30]). Figure 2(a) shows the schematic of the width pattern in which the gradient of widths is reversed periodically along the waveguides extension on z direction. For such array with $N = 65$ waveguides the resulting profile of waveguides propagation constants has been shown in Fig. 2(b) with $|\beta_i - \beta_{i+1}| = \delta\beta = 520m^{-1}$ and the pattern change at intervals $Z_B = 0.0063m$ along z direction that is related to the corresponding Bloch oscillation. While the difference of propagation constants of adjacent waveguides ($\delta\beta$) with respect to the propagation constant of an infrared beam (used in [30]) is small, we neglect the generation of backward traveling modes on each waveguide due to the mismatch of β's, and therefore suppose equal couplings for two nearest waveguides i.e. $J_{i,i+1} = J_{i+1,i}$ [30, 31]. The constant coupling for all adjacent waveguides is considered $J_{i,i+1} = 1240m^{-1}$ which requires the corresponding variation of waveguides' separation distances. We shine a Gaussian beam of $\phi(z = 0) = \exp(-(n - N/2)^2/10)$ at cross section $z = 0$ centered at waveguide number $n = N/2$ and numerically solve the coupled mode equations to find the intensity on each waveguide at different cross sections along z direction. We neglect the smallest propagation constant of waveguides for simplicity and suppose $\beta_i = i\delta\beta$ for $Z < Z_B$. We also add a nonlinear term $-6.5|\phi(z)|^2\phi(z)$ to the right side of the evolution equation which well describes the experimental situation in low power excitation for chosen parameters according to [29], and could be equivalent to the environmental noise effects in counterpart Schrodinger equation. Figure 2(c) shows the numerical values of intensities on all waveguides at different cross sections along z direction, where a_n is the amplitude of the electric field on waveguide n. It can be confirmed that the introduced width pattern of waveguides and the corresponding profile of propagation constants lead to uni-directional transport of Gaussian beams.

Morandoty et al [30] experimentally demonstrated some width-varied waveguide arrays, and assumed the ideal lossless case in which only one mode propagates on each waveguide. Our simulated network parameters (β and $J_{i,i+1}$) are chosen similar to those of their experiment, in which the widths of their 25 waveguides are varied from 2 to $3.4\mu m$. Supposing a linear increase of the guides' width with the number of guides, the maximum width of our chosen number of 65-guide array do not exceed $10.5\mu m$ which is the typical maximum width of a single-mode fiber. So all waveguides of the simulated 65-guide array could be considered single mode. In addition, one could decrease the minimum guides' width below $2\mu m$ to avoid any multimode propagation on all waveguides.

To check the non-reciprocity of these networks, we first note that these waveguide arrays should be always initiated from a middle site. This is due to the boundary limitation that spreads and reshapes the initial Gaussian beam which is expanded over several waveguides. To use such array as an isolator, one may consider a linear bench array and design input/output ports which are well-beyond the boundary waveguides. Now let's consider the upward-right propagating beam of Fig. 2 as case 1. If the array length would be an odd multiple of Z_B, launching a beam from the output port (top side) of the array (called case 2), is equivalent to launch a beam from the input port of the array with a reversed β variation pattern (case 3). According to simulations, in Fig. 2(c), the beam of case 3 perfectly travels upward-left, which is equivalent to the propagation of case 2 beam towards downward-right. By comparing cases 1 and 2, and taking into account that

Optics EXPRESS

the array length of Fig. 2 is $Z = 3Z_B$, the perfect right-azimuthal non-reciprocity of waveguides array of Fig. 2 is confirmed.

Such arrays could be also implemented by quantum site networks. The quantum nodes that are the counterpart elements of waveguides should undergo a time dependent self-energy profile as that of the propagation constants in Fig. 2(b) to yield non-reciprocal transport of energy excitations.

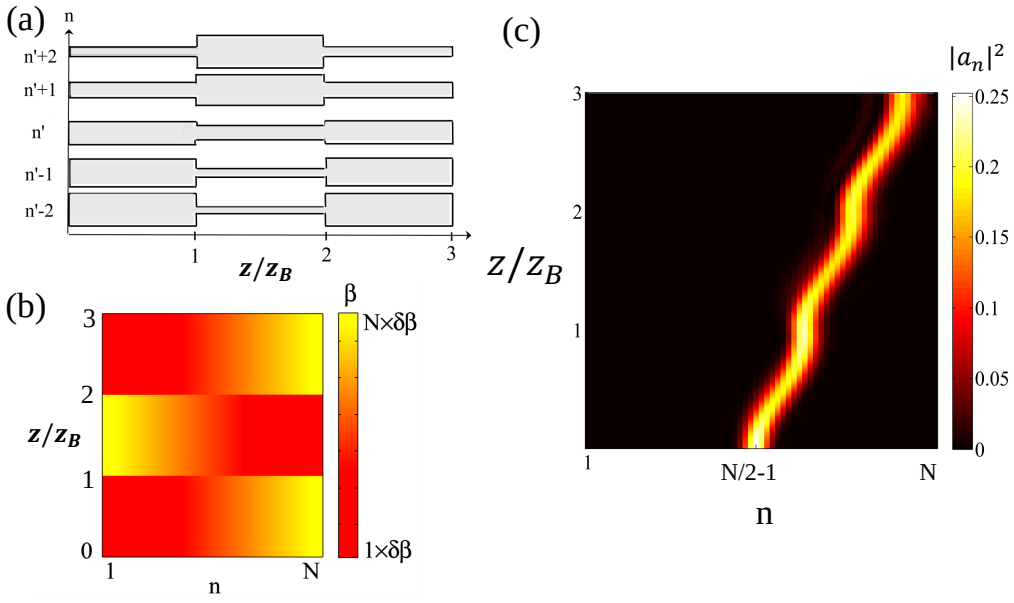

Fig. 2. Directed wave transport achieved through a width-patterned array of $N = 65$ waveguides exposed to a Gaussian beam of $\phi(z = 0) = \exp(-(n - N/2)^2/10)$. Graph (a) shows the schematic of the proposing width pattern array with waveguides indexed n extended along Z axis where $Z_B = 0.0063m$. The spatial modulation of the propagation constants of waveguides are shown in graph (b) where $|\beta_i - \beta_{i+1}| = \delta\beta = 520m^{-1}$. Same couplings of adjacent waveguides of $J_{i,i+1} = 1240m^{-1}$ are considered which could be achived by adjusting the nearest guides separations. Graph (c) represents the numerical simulation of intensity $|a_n|^2$ on waveguide n along Z direction which confirms the uni-directed transport of a Gaussian beam through such width patterned arrays.

2.2. *Ring networks*

In the previous subsection we focused on uni-directional transport in linear arrays. Now we follow the same procedures for ring networks to achieve directed chiral transport, and propose the designs as non-magnetic optical/quantum circulators. As the first example, we consider a time modulated dynamic network of nine sites each moving along a curve on a circular path. Figure 3(a) shows a schematic of such network where the first site is fixed at $(x_1 = 1, y_1 = 0)$ and the other sites are oscillating on a ring centered at the origin. The time variation of the angles subtended by each site is shown in Fig. 3(b). Next nearest sites are dipolar coupled to each other i.e. $J_{i,i+1} = 1/r^3_{i,i+1}$ where $r_{i,i+1}$ is the distance between the sites i and $i + 1$, and the site energies are considered to vanish ($\omega_i = 0$). Figure 3(c) shows the evolution of an energy excitation initially injected at the first site. It can be seen that it continually travels along the neighboring pair of sites through the ring and returns to the first site. This behaviour is due to the designed dynamics of the pair of sites so that the initial energy excitation evolves to a superposition state of two close

Optics EXPRESS

sites and so is being handed over the ring to reach the first site. Figure 4(d) shows the evolution of the initial excitation in a longer duration.

To explain the azimuthal non-reciprocity of such dynamic networks, we note that by launching an energy excitation on any intermediate site, the pair transportation mechanism would carry that around the ring in a clockwise or counterclockwise way which is determined by the position pattern of sites. Such energy circulating networks could be implemented by cold atoms in dynamically controlled optical lattices [23, 24], or equivalently curved waveguide arrays on cylindrical substrates. As the second example of uni-directed chiral transport, we consider a

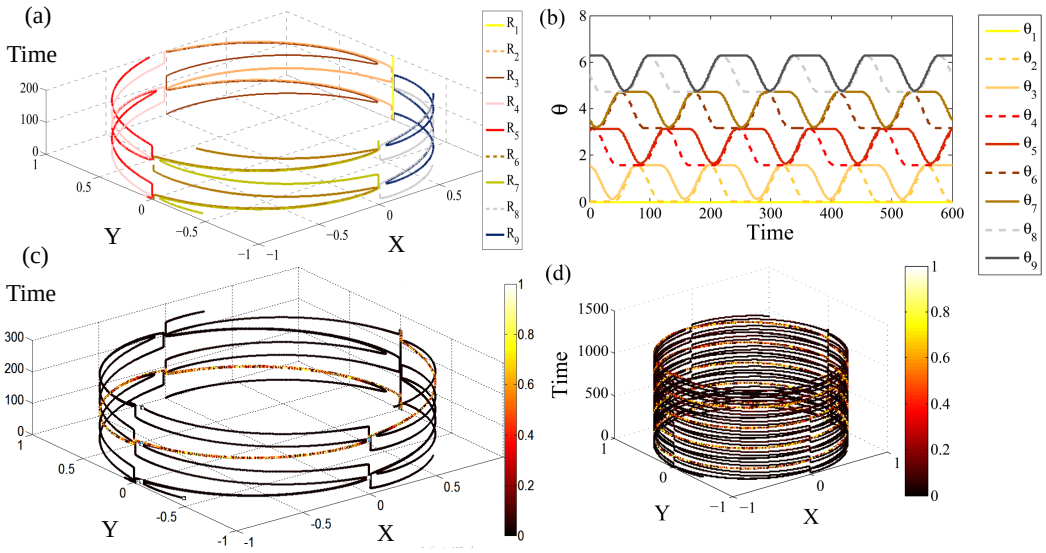

Fig. 3. A non-magnetic optical circulator via a dynamically controlled ring network of nine sites. Graph (a) shows the trajectories of nine sites ($R_{i;i=1-9}$) in time that are initially located equidistantly on a circle on xy plane centered at the origin. The first site is fixed in time at ($x_1 = 1, y_1 = 0$). Graph (b) shows the modulation of angles trajectories (in radian) for each site in time. Graphs (c) and (d) represent the dynamics of the probability of energy excitation initially launched at site 1, through the network in shorter and longer time intervals, respectively. The color scale is the total probability of energy excitaiton ($|\psi|^2$) which varies in time at the location of each site.

waveguide array with a specific profile for propagation constants. In section 2.1, directed transport was achieved in a linear waveguide array by designing the waveguides' widths as schemed in Fig. 2(a), which is equivalent to fashion the propagation constants profile as shown in Fig. 2(b). As discussed in [29] one way to achieve such profile is to periodically flipping the direction of an applied electric field across a waveguide array of photorefractive materials. The electric field creates a gradual increase of refractive indices (and consequently the propagation constants) along the azimuthal direction of waveguide array leading to Bloch oscillations. By flipping the direction of electric force (or reversing the upward trend of β pattern) an initially launched Gaussian beam could be directed non-reciprocally across the array. If the parallel waveguides are separated by distance d then the increase of propagation constants over nearest waveguides is $|\beta_i - \beta_{i+1}| = \delta\beta = Fd$ where F is the magnitude of the electric force [29]. By supposing $\hbar = 1$ the distance and force could be considered in Planck units. In this section, to achieve a chiral and non-reciprocal transport via waveguides array on a cylindrical substrate, we propose a new width pattern to obtain a linear increase of propagation constants from the last waveguide to the first

Optics EXPRESS

one. The schematic of the new width profile and the corresponding cylindrical array are shown in Fig. 4(a). The left graph indicates that at each increment along the z axis the waveguides widths vary linearly and follow a sawtooth function to maintain a continuous increase of propagation constants from the last guide towards the first one. The rate of width variation along the z and n axes are related to the velocity of corresponding Bloch waves (V_B). The right graph of Fig. 4(a) shows a schematic of an array on a cylindrical substrate where an input Gaussian beam reaches at the end of the network after 2.25 round trips. To simulate this width-patterned array, we consider an array of $N = 200$ waveguides on a cylindrical substrate and apply a Gaussian beam of $\phi(z = 0) = \exp(-(n - N/2)^2/100)$ centered at waveguide number $n = N/2$. We consider next-nearest-waveguides couplings as $J_{i,i+1} = J_{i+1,i} = \Delta/4$ where $\Delta = 0.994$. The velocity of the corresponding Bloch wave is $V_B = 2\gamma/(z_B/2) = 0.165$, where $\gamma = \Delta/F$ is the amplitude of the Bloch wave along the waveguide numbers, $z_B = 2\pi\hbar/(Fd)$ is the wavelength of Bloch oscillation, and $F = 0.005$ and $d = 2\pi$ are the magnitude of the applied electric force and waveguides separations in a counterpart optoelectric waveguide array, respectively. While assumed $\hbar = 1$, all quantities could be considered in Planck units. Figure 4(b) shows the corresponding β profile of such width-patterned arrays where $\beta \in [\delta\beta, N\delta\beta]$ and $\delta\beta = (-1)^{\lfloor(z/(z_B/4))\rfloor}Fd$ that flips sign at length intervals $z_B/4$. The variation of propagation constants along z direction is considered $\delta\beta/\delta z = V_B$ to keep the increasing trend of $\delta\beta$ at the position of propagating beam, and minimize the power loss after each round trip. Figure 4(c) shows the simulated intensity on each waveguide ($|a_n|^2$) along z direction. It can be seen that chiral transport of an initial Gaussian beam is achieved via the proposed modulation of propagation constants shown in Fig. 4(b).

To verify the azimuthal non-reciprocity, we first notify that according to simulations, there are two cases that reverse the chiral direction of a Gaussian beam launched at a unique input port. In the first case, the direction is perfectly reversed if the following conditions are satisfied: Reversing the slope of β variation pattern of Fig. 4(b), as well as reversing the sign of $\delta\beta$ within the first $z_B/4$ interval ($0 \leq z < z_B/4$) i.e. $\delta\beta = (-1)^{\lfloor(z/(z_B/4))\rfloor+1}Fd$. In the second case, the initial sign of $\delta\beta$ would reverse within the first interval, however, the β slope is not reveresed which yields an inefficient propagation towards the reversed chiral direction. Now we compare the directions of the propagating Gaussian beams launched on both sides of the circulator of Fig. 4. The slope of β variation pattern (Fig. 4(b)) for both ways are similar, which satisfies one condition of the inefficient chiral reversibility. If the length of the cylindrical circulator would be slightly less than an odd multiple of $z_B/4$ i.e. $\lfloor z/(z_B/4)\rfloor = (2n)$, the sign of $\delta\beta$ within the initial interval along z axis for both input and output launched beams would be similar. So both waves would have identical environemnts and travels towards their outward right side. As the input beam of Fig. 4(c) propagates upward right, the beam launched at the output port propagates downward left of Fig. 4(c), yielding a perfect azimuthal reciprocity. On the other hand, for cylinder lengths of slightly less than an even multiple of $z_B/4$, i.e. $\lfloor z/(z_B/4)\rfloor = (2n + 1)$, the sign of $\delta\beta$ is reversed for a launched beam from the opposite side, and so both conditions of inefficient chiral reversibility are satisfied. Since the length of the introduced circulator of Fig. 4(c) is an even multiple of $z_B/4(z = 60z_B/4)$, the conditions of inefficient chiral reversibility are almost satisfied for an output launched beam with respect to an input launched beam. While the input beam propagates upward right in Fig. 4(c), the output launched beam propagates downward right on the same figure, yielding azimuthal non-reciprocity of the network of Fig. 4(c).

Such proposed chiral beam transporters could be built by direct laser-writing and 3D printing [25,26] and be used as non-magnetic optical circulators in photonic circuits. While magnetic Faraday optical circulators have only a few output ports, these cylindrical arrays could change the direction of an incident Gaussian beam for an arbitrary angle via the manipulation of network parameters. In addition, the proposed width-patterned networks could be used as optical retarders, and the torus version of such cylindrical networks could be studied as beam trappers for optical computing applications. The formerly proposed dynamic ring networks could be also used as

Optics EXPRESS

quantum memories or energy excitation trappers as well as non-reciprocal energy transporters towards arbitrary angles.

Quantum nodes in ring arrays could also implement the introduced circulator of Fig. 4 by adjusting the pattern of site energies in time as that of the propagation constants along z axis shown in Fig. 4(b).

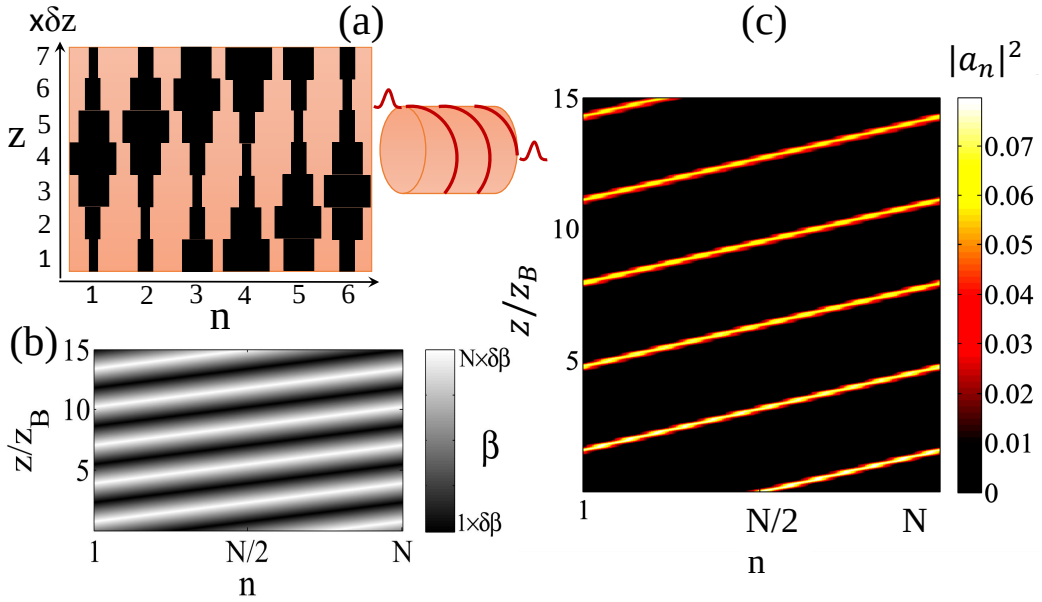

Fig. 4. A non-magnetic optical circulator made of a cylindrical width-patterned waveguide array for directed and non-reciprocal chiral transfer of Gaussian beams. Graph (a) shows the schematic of a width varying waveguide array (left part) which is designed on a cylindrical shell (right part). Graph (b) shows the profile of propagation constants as a function of waveguide number n along z direction where $n \in [1, N = 200]$, $\delta\beta = (-1)^{\lfloor (z/(z_B/4)) \rfloor} Fd$, $F = 0.005$, $d = 2\pi$, and the nearest guides' couplings of $J_{i,i+1} = J_{i+1,i} = 0.2485$. Graph (c) represents the numerical solutions of intensities accross a cylindrical waveguide array that is initially launched by a Gaussian beam of $\phi(z = 0) = \exp(-(n - N/2)^2/100)$. It could be confirmed that the incident Gaussian beam would uni-chirally and non-reciprocally propagate around the cylinderical shell. The chiral direction could be inversed via mirroring the $\beta(n, z)$ pattern with respect to line $n = 1$, and reversing the starting sign of $\delta\beta$. By adjusting network parameters like cylinder length or $\beta(n, z)$ profile, such networks could deviate a Gassian beam for an arbitrary angle to be used as a non-magnetic optical circulator.

3. Conclusion

We introduced four different linear and ring networks implemented by dynamic sites, curved, and width-patterned parallel waveguides for non-reciprocal and uni-directional/uni-chiral transport of energy excitations or Gaussian beams. Since each introduced system has a counterpart implementation, i.e. dynamic sites or waveguides array, eight non-reciprocal and uni-directional networks have been potentially presented. In linear and ring dynamic sites (curved waveguides) the initial energy excitation would uni-directly transfer through the network via oscillating between closely positioned pair of sites. One-way transport of Gaussian beams is via tunneling across specific width-patterned waveguides array that are equivalent to site networks with dynamic energies of sites. Such non-magnetic networks could be used in linear, ring, planer, and cylindrical geometries as quantum/optical diodes and circulators in quantum/photonic circuits.

Optics EXPRESS

Funding

ARC Centre of Excellence for Engineered Quantum Systems; ARC Project No. CE110001013.